A Monomer-to-Dimer Shift in a Series of 1:1 Ferric Dihydroxamates Probed by Electrospray Mass Spectrometry

M. Tyler Caudle,† Robert D. Stevens,‡ and Alvin L. Crumbliss*,†

Department of Chemistry, Duke University, Box 90346, Durham, North Carolina 27708-0346, and Division of Genetics and Metabolism, Department of Pediatrics, Duke University Medical Center, Durham, North Carolina 27710

Received February 17, 1994®

Electrospray mass spectrometry (ESMS) was used to determine the stoichiometry of a series of 1:1 iron(III) complexes with model dihydroxamic acids H_2L, $[CH_3N(OH)C(O)]_2(CH_2)_n$, and with the natural dihydroxamate siderophore rhodotorulic acid, RA. Parent (or complex molecular ion) peaks were observed at *m/z* 314, 286, 258, and 230 for the model complexes where $n = 8, 6, 4, 2$, respectively, and at *m/z* 398 for the analogous RA complex. The isotope distribution patterns in the ESMS strongly suggest that the model complexes exist in a dimeric form, $Fe_2L_2^{2+}$, when $n = 2, 4$. A monomeric structure, FeL^+, is consistent with the isotope distribution patterns for the ESMS of the model complex when $n = 8$, and for the RA complex. The model complex, $n = 6$, exhibits more complicated ESMS data, suggesting that both monomer and dimer exist in solution. Molecular mechanics computational studies performed on the model complexes give a relative conformational strain energy, E_m, of 9, 10, 20, and 56 kcal/mol for $n = 8, 6, 4, 2$, respectively, when a monomeric structure is assumed. When a dimeric structure is assumed for the model complexes, the relative strain energy, E_d, is 14, 13, 13, and 12 kcal/mol. For the RA complex, relative strain energies are 10 and 16 kcal/mol for the monomeric and dimeric structures, respectively. The shift from monomer to dimer as n is decreased is discussed in terms of the increase in conformational strain enthalpy in the monomeric structure as n is decreased.

Introduction

N-terminal synthetic model dihydroxamic acids, **I**, have been extensively studied as models for the naturally occurring iron(III) chelator rhodotorulic acid (RA), **II**, due to their ease of preparation and to the variety which can be incorporated into the structure.[1-11] Rhodotorulic acid functions as a siderophore, binding and transporting iron in *Rhodotorula pilimanae*.[11-14] The structural similarity between the model compounds and RA make a study of the coordination chemistry and transport properties of the model compounds useful in the elucidation of the mechanism of RA-mediated iron transport.

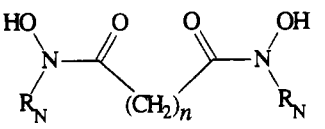

I

$R_N = Me$

$n = 8$(**a**), 6(**b**), 4(**c**), 2(**d**)

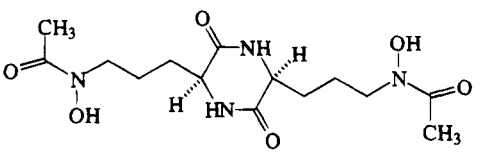

II

The coordination chemistry of iron complexes with RA and with synthetic dihydroxamic acids has been explored in detail.[1-14] The characteristic equilibria involved in the formation of the fully coordinated iron complex are shown in eqs 1 and 2. The bifunctional nature of the dihydroxamic acids make

$$Fe^{3+} + H_2L \rightleftharpoons FeL^+ + 2H^+ \quad (1)$$

$$2FeL^+ + H_2L \rightleftharpoons Fe_2L_3 + 2H^+ \quad (2)$$

them interesting ligands due to their ability to form bimetallic iron(III) complexes of formula Fe_2L_3 at excess ligand and pH > 4. This complex stoichiometry has been established to exist for RA as well as for model dihydroxamic acids.[1-14] A fundamental problem arises, however, in the characterization of the 1:1 complex, FeL, which forms at pH 3 and below. Two possible structures for the 1:1 complex are shown in Scheme 1.

Potentiometric and spectrophotometric evidence has been used to propose that the 1:1 complex formed below pH 3 is

* Author to whom correspondence should be addressed.
† Duke University.
‡ Duke University Medical Center.
® Abstract published in *Advance ACS Abstracts*, November 1, 1994.
(1) Barclay, S. J.; Huynh, B. H.; Raymond, K. N. *Inorg. Chem.* **1984**, *23*, 2011.
(2) Barclay, S. J.; Riley, P. E.; Raymond, K. N. *Inorg. Chem.* **1984**, *23*, 2005.
(3) Scarrow, R. C.; White, D. L.; Raymond, K. N. *J. Am. Chem. Soc.* **1985**, *107*, 6540.
(4) Brown, D. A.; Geraty, R.; Glennon, J. D.; Choileain, N. N. *Inorg. Chem.* **1986**, *25*, 3792.
(5) Das, M. K.; Chaudhury, K.; Roy, N.; Sarkar, P. *Transition Met. Chem.* **1990**, *15*, 468.
(6) Santos, A. M.; Esteves, A.; Vaz, M. C. T.; Goncalves, M. L. S. S. *J. Chem. Soc., Dalton Trans.* **1993**, 927.
(7) Evers, A.; Hancock, R. D.; Martell, A. E.; Motekaitis, R. J. *Inorg. Chem.* **1989**, *28*, 2189.
(8) Chaubet, F.; Nguyen van Duong, M.; Gref, A.; Courtieu, J.; Crumbliss, A. L.; Gaudemer, A. *Tetrahedron. Lett.* **1990**, *31*, 5729.
(9) Chaubet, F.; Van Duong, J.; Courtieu, J.; Gaudemer, A.; Gref, A.; Crumbliss, A. L. *Can. J. Chem.* **1991**, *69*, 1107.
(10) Chaubet, F.; Duong, K. N. V.; Gref, A.; Courtieu, J.; Crumbliss, A. L.; Caudle, M. T.; Gaudemer, A. *Can. J. Chem.*, in press.
(11) Carrano, C. J.; Cooper, S. R.; Raymond, K. N. *J. Am. Chem. Soc.* **1979**, *101*, 599.
(12) Carrano, C. J.; Raymond, K. N. *J. Bacteriol.* **1978**, *136*, 69.
(13) Müller, G.; Isowa, Y.; Raymond, K. N. *J. Biol. Chem.* **1985**, *260*, 13921.
(14) Müller, G.; Barclay, S. J.; Raymond, K. N. *J. Biol. Chem.* **1985**, *260*, 13916.

0020-1669/94/1333-6111$04.50/0

Scheme 1. Two Possible Structures for a General 1:1 Ferric Dihydroxamate Complex[a]

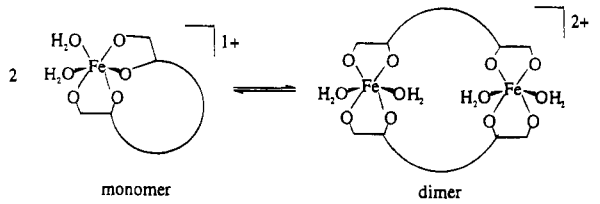

[a] The orientation of the hydroxamate groups is not shown.

monomeric, Scheme 1, in all cases where the chain length separating the hydroxamate groups ranges from 2 to 10 methylene units.[1-14] However, it is conceivable that a bifunctional ligand such as the dihydroxamic acids could form a dimeric iron complex, assuming a suitable driving force were provided for eq 3. This reaction would be impossible to monitor

$$2FeL^{+} \rightleftharpoons Fe_2L_2^{2+} \quad (3)$$

by ordinary spectrophotometric or potentiometric means since the observable quantity is dependent only on the concentration of iron and on the metal-to-ligand ratio. In other words, such experiments are not conclusive evidence for the presence of monomer or dimer since the data can be intepreted in terms of either. In fact, based on available potentiometric or spectrophotometric data any oligomer with a 1:1 metal-to-ligand ratio would fit the experimental data. The characterization of this species is a significant problem in that the rate and mechanism by which iron is removed from a natural or model dihydroxamate siderophore complex, Fe_2L_3, *in vivo* or *in vitro*, may be strongly dependent on whether the proposed 1:1 intermediate is monomeric or dimeric.[15] A chain-length dependence and a pH dependence, which may be related to the nature of the 1:1 complex, has been observed in the uptake of model ferric dihydroxamate complexes, Fe_2L_3, by *R. pilimanae*.[12,14] Chain length is also of relevance in consideration of the structure of the more common trihydroxamate siderophores, insofar as the chain length separating the iron binding sites affects the structure, stability, and lability of these complexes as well.[15-17]

Electrospray mass spectrometry (ESMS)[18,19] has recently been used to elucidate structural and solution properties of inorganic complexes in solution.[20-28] A preliminary communication has reported the use of ESMS to show that an *N*-methyldihydroxamic acid forms a monomeric complex when eight methylene units (**Ia**) separate the hydroxamate groups, but exclusively dimer forms when only two methylene units (**Id**) separate the hydroxamate groups.[29] It is apparent that there must be some system having between two and eight methylene units separating the iron binding sites, where the crossover from a monomer to dimer structure occurs. In this paper, we have explored the N-terminal N-methyldihydroxamic acid-iron(III) system in further detail using ESMS, including systems having six and four methylene units (**Ib** and **Ic**), in an effort to experimentally observe the transition from monomer to dimer. In addition, this work includes an ESMS study of the 1:1 iron(III) complex with RA (**II**) in order to determine whether this siderophore complex forms the 1:1 monomer or dimer.

Experimental Section

Materials and Equipment. The preparation of the ligands **Ia-d** is described elsewhere.[30] Rhodotorulic acid, **II**, was obtained from Sigma (97%) and used as received. Solutions for ESMS analysis were prepared by combining equimolar amounts of Fisher analytical grade ferric chloride, $FeCl_3 \cdot 6H_2O$, and the desired ligand in twice distilled water to give $[Fe^{3+}]_{tot} = [L^{2-}]_{tot} \approx 0.50$ mM. The pH of the solution was adjusted to about 2.3 by dropwise addition of concentrated HCl while stirring vigorously. Due to the small amount of RA available for this study, its concentration was estimated from the equivalence point of a potentiometric pH titration curve obtained for a stock solution of the uncomplexed ligand. This stock solution was then used to prepare the iron complex solution for analysis.

UV/visible spectra of the complexes were measured using a Hewlett-Packard 8451 diode array spectrophotometer. The pH measurements were made using a Corning 250 pH/ion meter and a Corning General Purpose glass electrode. The ESMS measurements were made using a Fisons Instruments VG BIO-Q quadrupole mass spectrometer run in positive ion mode and equipped with a pneumatically assisted electrostatic ion source operating at atmospheric pressure. Molecular mechanics modeling computations were performed using a Silicon Graphics IRIS workstation using SYBYL 6.0a.

ESMS Measurements. The UV/visible spectrum of each solution was measured prior to ESMS analysis. ESMS measurements were performed on mixtures of the iron complex solutions with acetonitrile in varying proportions. Acetonitrile is added as a volatile but noncoordinating solvent to ease desolvation of the complex. No dependence on concentration was observed in the shape of the mass spectrum over the concentration range studied (0.05-0.50 mM). A mobile phase of 1:1 (v/v) CH_3CN/water and a sample flow rate of 6 μL/min was used for LC injection into the ES ion source. The mass spectrometer was operated at unit mass resolution and the mass scale was calibrated using polyethylene glycol.

Molecular Modeling Studies. The SYBYL 6.0a implementation of the Tripos 5.2 valence force field[31] was used in molecular mechanics studies on the 1:1 iron complexes. Additional force field parameters were added to the standard Tripos values to account for the iron center.[32] In addition, some standard equilibrium bond distances and angles were modified somewhat based on crystallographic data for iron hydroxamate complexes.[16] The extensions to the standard force field are listed in Table 1.[33] Electrostatic contributions to the steric energy were neglected. The lowest energy conformation was found by a random conformational search of the heavy atoms such that there was a 96.9% probability that all of the valid conformation space had been probed. A gradient convergence criterion of 0.05 kcal/mol was used to determine convergence for a given conformation. Hydrogens were then included and a final minimization performed to find the lowest energy conformation.

Results

ESMS Studies. ESMS data for a representative ferric dihydroxamate complex, H_2L = **Ia**, is shown in Figure 1A.

(15) Crumbliss, A. L. In *CRC Handbook of Microbial Iron Chelates*; Winkelmann, G., Ed.; CRC Press: New York, 1991; Chapter 7, pp 177-233.
(16) van der Helm, D.; Jalal, M. A. F.; Hossian, M. B. In *Iron Transport in Microbes, Plants, and Animals*; Winkelmann, G., van der Helm, D.; Neilands, J. B., Eds.; VCH: Weinheim, Germany, 1987; Chapter 9.
(17) Yakirevitch, P.; Rochel, N.; Albrecht-Gary, A.; Libman, J.; Shanzer, A. *Inorg. Chem.* **1992**, *32*, 1779.
(18) Fenn, J. B. *J. Am. Soc. Mass Spectrom.* **1993**, *4*, 524.
(19) Kebarle, P.; Tang, L. *Anal. Chem.* **1993**, *65*, 972A.
(20) Colton, R.; Bruce, D. J.; Potter, I. D.; Traeger, J. C. *Inorg. Chem.* **1993**, *32*, 2626.
(21) Colton, R.; Tedesco, V.; Traeger, J. C. *Inorg. Chem.* **1992**, *31*, 3865.
(22) van den Bergen, A.; Colton, R.; Percy, M.; West, B. O. *Inorg. Chem.* **1993**, *32*, 3408.
(23) Bond, A. M.; Colton, R.; D'Agostino, A.; Harvey, J.; Traeger, J. C. *Inorg. Chem.* **1993**, *32*, 3952.
(24) Colton, R.; Traeger, J. C. *Inorg. Chim. Acta* **1992**, *201*, 153.
(25) Colton, R.; Dakternieks, D. *Inorg. Chim. Acta* **1993**, *208*, 173.
(26) Colton, R.; Kläui, W. *Inorg. Chim. Acta* **1993**, *211*, 235.
(27) Cantry, A. J.; Colton, R. *Inorg. Chim. Acta* **1994**, *215*, 179.
(28) Haselwandter, K.; Dobernigg, B.; Beck, W.; Jung, G.; Cansier, A.; Winkelmann, G. *BioMetals* **1992**, *5*, 51.
(29) Caudle, M. T.; Stevens, R. D.; Crumbliss, A. L. *Inorg. Chem.* **1994**, *33*, 843.
(30) Caudle, M. T.; Cogswell, L. P.; Crumbliss, A. L. *Inorg. Chem.* **1994**, *33*, 4759.
(31) Clark, M.; Cramer, R. D. I.; Van Opdenbosch, N. *J. Comput. Chem.* **1989**, *10*, 982.
(32) Hay, B. *Coord. Chem. Rev.* **1993**, *126*, 177.
(33) See paragraph at end of paper for information on supplementary material deposited.

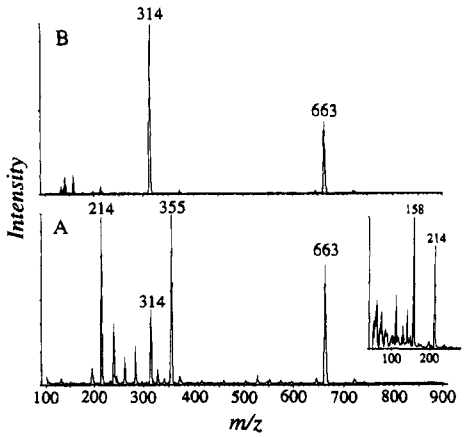

Figure 1. ESMS of the iron(III) complex with **Ia**. $[Fe^{3+}]_{tot} = [L^{2-}]_{tot}$ = 0.52 mM. pH = 2.3 (HCl). Solvent: 1/1 (v/v) CH_3CN/H_2O. Mobile phase 1/1 (v/v) CH_3CN/H_2O. Key: (A) B1 = 26 V. (B); B1 = 46 V. Inset: background ESMS. pH = 2 (HCl). Solvent: 1/1 (v/v) CH_3CN/H_2O. Mobile phase: 1/1 (v/v) CH_3CN/H_2O. B1 = 42 V.

Table 2. ESMS Data for the Iron(III) Dihydroxamate Complexes[a]

ligand	EFW[b]	m/z[c]	m/z[d]
Ia	314	314	355, 663
Ib	286	286	327, 607
Ic	258	258	551
Id	230	230	495
RA	398	398	

[a] $[Fe^{3+}]_{tot} = [L^{2-}]_{tot}$ = 0.50 mM. pH = 2.3 (HCl). Solvent: 1/1 (v/v) CH_3CN/H_2O. Mobile phase: 1/1 (v/v) CH_3CN/H_2O. B1 = 29–32 V. [b] Theoretical empirical formula weight of the 1:1 ferric dihydroxamate complex. [c] Parent ion peak. [d] Other peaks observed in the ESMS.

Several features of interest are observed. The intense signals at *m/z* 314, 355, and 663 can be assigned to iron-containing complexes with **Ia**, Table 2. Little fragmentation of the actual iron(III) complex occurs, and most peaks below the *m/z* of the parent ion can be ascribed to electrospray background ions. Collisionally induced fragmentation studies on **Ia** have shown that fragmentation of the free ligand can contribute to the peak at *m/z* 214.[29] However, this peak is also very intense in the background spectrum of pH 2 HCl, Figure 1 (inset). In fact, the intense background ion artifacts at *m/z* 214 and below in aqueous HCl media limit the analytical usefulness of our data below this threshold. ESMS data from *m/z* 100 to *m/z* 900 are are shown for the iron complexes with **Ib–d** and RA in Figures 2–5.[33]

The mass-to-charge ratios (*m/z*) for the parent peak (or complex molecular ion peak)[28] in the mass spectrum of each complex are listed in Table 2. In some cases, additional prominent peaks appear having *m/z* greater than the parent peak, and are due to formation of clusters or adducts, as discussed below. Peaks with *m/z* below the parent ion, due to fragmentation of the complex or residual ligand, will not be further interpreted here, due to background interference at low *m/z*. Because the monomer or dimer with a given ligand will have identical *m/z*, a simple inspection of *m/z* for the parent ion peak is not sufficient to distinguish whether that complex is the monomer, FeL^+, or the dimer, $Fe_2L_2^{2+}$. However, the isotope distribution pattern is unique for a monomer or dimer, and can be used to determine the stoichiometry of a given 1:1 ferric dihydroxamate complex.[29]

The iron complex with **Ia** gives an ESMS parent peak centered at *m/z* 314, Figure 6A, as expected. An isotope peak due to the presence of ^{13}C and ^{57}Fe appears one unit higher. More importantly, a signal appears two units below the parent

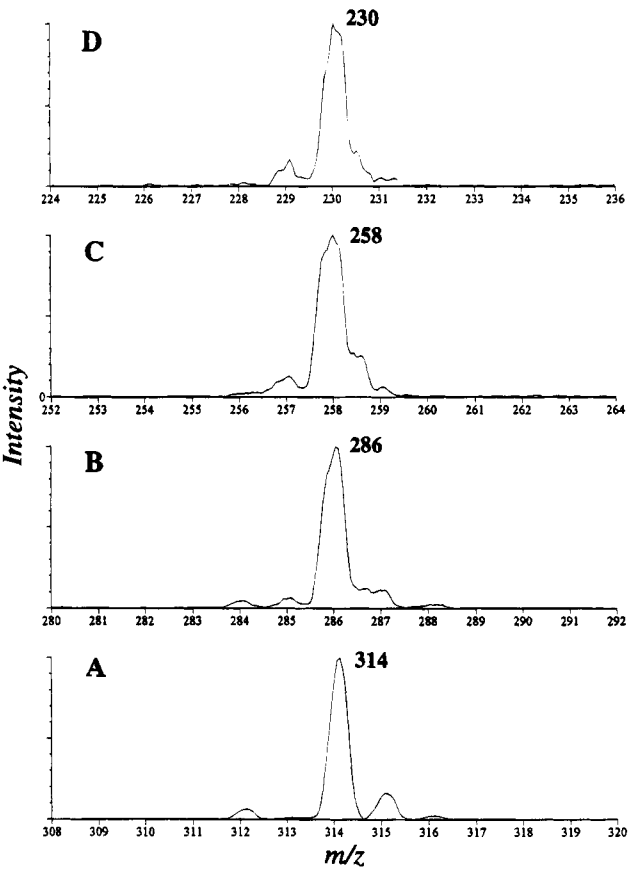

Figure 6. ESMS of the model 1:1 ferric dihydroxamate complexes. $[Fe^{3+}]_{tot} = [L^{2-}]_{tot}$ = 0.50 mM. pH = 2.3 (HCl). Solvent: 1/1 (v/v) CH_3CN/H_2O. Mobil phase: 1/1 (v/v) CH_3CN/H_2O. B1 = 29–32 V. Key: (A) H_2L = **Ia**; (B) H_2L = **Ib**; (C) H_2L = **Ic**; (D) H_2L = **Id**.

peak, due almost exclusively to the presence of the ^{54}Fe isotope. It has been shown that this pattern is characteristic of the 1:1 monomer FeL^+, H_2L = **Ia**.[29] In general, the presence of a fairly intense isotope peak two units below the parent peak is characteristic of the mass spectrum for a singly-charged iron-containing complex.[29]

Figure 6D shows the ESMS parent peak of the iron complex of **Id**, *m/z* 230. There is a fairly intense isotope peak only one unit below the parent peak, *m/z* 229, instead of appearing two units below. No reasonably intense ^{13}C isotope peak exists at *m/z* 231 though the parent peak is broadened and asymmetric with respect to Figure 6A. The lower resolution between *m/z* 230 and 231 suggests that the ^{13}C peak is shifted toward the parent peak in Figure 6D. The isotope distribution pattern is compressed by a factor of two compared to Figure 6A, consistent with charge doubling in the **Id** complex. Therefore, the mass of the ion in Figure 6D must be 460 amu. These observations can be consistent only if Figure 6D is the spectrum of a doubly-charged dimer $Fe_2L_2^{2+}$. Spectrum simulation based on $Fe_2L_2^{2+}$ fits Figure 6D very well,[29] whereas a simulation based on the singly-charged monomer does not produce an isotope distribution consistent with experiment.

The mass spectrum of the iron complex with **Ic**, Figure 6C, has an isotope distribution pattern similar to 6D, though centered instead at *m/z* 258. The ^{54}Fe isotope peak appears at *m/z* 257. The ^{13}C peak exists at *m/z* 258.5 and is somewhat more pronounced than in Figure 6D, due to the larger number of carbons in **Ic** *vs* **Id**. The same arguments concerning the iron complex of **Id** above may be used to assign the stoichiometry of the complex with **Ic** as $Fe_2L_2^{2+}$.

The ESMS data for the iron(III) complex of **Ib**, Figure 6B, are more complicated and cannot be explained on the basis of

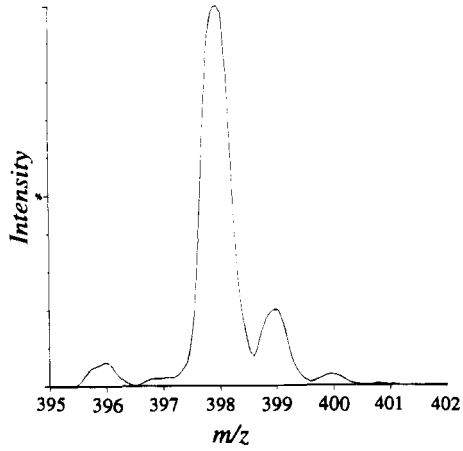

Figure 7. ESMS of the 1:1 ferric rhodotorulate complex. $[Fe^{3+}]_{tot} = [RA^{2-}]_{tot} = 0.50$ mM. pH = 2.3 (HCl). Solvent: 1/1 (v/v) CH_3CN/H_2O. Mobile phase: 1/1 (v/v) CH_3CN/H_2O. B1 = 30 V.

a single complex ion. The parent peak is at *m/z* 286, as expected. However, there are well defined isotope peaks at *m/z* 284 and 285. The signal at *m/z* 287 can be assigned to ^{13}C contributions, but there is also a spectral feature between *m/z* 286 and 287. Therefore, Figure 6B has spectral features characteristic of both the monomer and the dimer. This suggests a system in which both the monomeric and the dimeric complexes coexist in equilibrium. The observed spectrum is then the weighted sum of the spectrum due to the monomer complex and the compressed spectrum due to the dimer complex. The **Ib** iron complex represents a "crossover" system between those which are purely monomeric ($n = 8$) and purely dimeric ($n = 2, 4$). It is, in theory, possible to calculate the ratio of monomer to dimer in this system by a line shape analysis. However, the information gained may be of little use in extrapolating the ratio observed in the mass spectrum with that existing in solution, since the mechanism of ESMS is complicated and not fully understood at present.[18,19]

Figure 7 shows the isotope distribution pattern for the parent peak (*m/z* 398) in the mass spectrum of the 1:1 iron complex with rhodotorulic acid, **II**. The parent peak is not as intense as for the model complexes, Figure 5,[33] due to the delicate nature of this system which may lead to some fragmentation. The ^{54}Fe isotope peak is two units below the parent at *m/z* 396 and the ^{13}C peak is one unit above at *m/z* 399. The isotope distribution pattern is, therefore, similar to that observed for the iron complex with **Ia**, and is consistent with a monomeric complex. This confirms previously published reports on the coordination chemistry of ferric rhodotorulate complexes that propose a monomeric structure for the 1:1 complex.[11] There is a very slight asymmetry on the upper side of the peak at 398, and a small feature at 397, suggesting that a small amount of dimer may form in this system. However, the intensity of these features is low and the monomer is largely favored for RA.

ESMS obtained on the iron(III) complex with **Ia** at B1 = 29 V, Figure 1A, exhibits a signal at $m/z = m_{parent} + 41 = 355$. This has been ascribed to an acetonitrile adduct either formed in the ionization process or pre-existing in solution.[29] This adduct should be quite weak since acetonitrile is only a slightly coordinating solvent for iron(III). When B1 is increased to 46 V, this signal disappears, Figure 1B, consistent with disruption of a weak adduct at higher accelerating potentials. The iron(III) complexes with **Ib** exhibit similar ESMS behavior, Figure 2,[33] having an $m_{parent} + 41$ peak at *m/z* 327 when B1 = 42 V. The acetonitrile adduct is not observed in the ESMS of the 1:1 $FeRA^+$ monomeric complex even at B1 = 30 V.

Another interesting aspect of the ESMS data, Table 2, is that even at low accelerating potential, the complex ions have been dehydrated, even to removal of all coordinated waters. Furthermore, no water containing species are observed in the mass spectrum under any of our conditions. The loss of coordinated waters from iron(III) complexes in ESMS sources has been reported for other iron(III) cations.[22] This most likely stems from the lability imparted to coordinated water upon addition of a hard negative donor to the inner coordination shell of the iron(III) complex. The complete loss of coordinated water, and the observation of acetonitrile adducts, suggest that the acetonitrile adduct is bound by some mode different from, or in addition to, coordination. If coordination to the iron were the primary interaction holding the acetonitrile adduct together, then we would expect to see water adducts as well, since water is more coordinating for iron(III) than acetonitrile.

The ESMS spectra of the model complexes with **Ia–d** show a signal at $m/z = 2m_{parent} + 35$, consistent with a stoichiometry of $Fe_2L_2Cl^+$(*m/z* 663, 607, 551, and 495 for the $n = 8, 6, 4, 2$ model systems, respectively). The isotope distribution patterns suggest a chloride containing dimer,[29] though the exact nature of the interaction with the chloride is uncertain. Since chloride is a coordinating ligand for iron(III), it may be attached directly to iron, either in a terminal or bridging mode. However, the observation that this signal is somewhat attenuated by increasing B1, Figure 1, suggests the possibility that the chloride containing dimer is simply an ion cluster held together by electrostatic forces. Such ion clustering has been observed with ESMS ion sources.[34,35] Another ambiguity concerns whether the dihydroxamate ligands are bridging two iron centers or whether this species is simply a cluster involving two monomer units. In the case of ligands **Ic** and **Id**, it seems most likely that the dihydroxamate ligands are in a bridging mode. However the lack of ESMS evidence for formation of a simple dimer without chloride when the ligand is **Ia** suggests that the chloride containing species at 663, Table 2, is simply a cluster of two monomers held together by a bridging chloride. This species is not observed for the 1:1 $FeRA^+$ species, even at B1 as low as 30 V.

Molecular Modeling Studies. Suitable crystals for X-ray analysis could not be grown so no X-ray crystallographic data exist for these complexes. The ESMS experiment gives no information as to the exact structure of the complex, but only establishes the stoichiometry of the complex. Therefore, molecular mechanics calculations were used to probe possible structures and relative energies for the monomeric and dimeric complexes.

The calculated minimum steric energies, E_m, assuming the monomer structure for the model complexes, show a monotonic increase as the chain length *n* is decreased, Table 3. According to the molecular mechanics model, this is associated with an increase in the angle bending and the torsional contributions in the monomer. There is minimal variation in the calculated steric energy, E_d, when a dimer structure is assumed for the complexes. For the hypothetical reaction, eq 3, the calculated energy change due to steric strain is given by $\Delta E_{calc} = E_d - 2E_m$, Table 3. The large decrease in ΔE_{calc} for the iron(III) complexes with **Ic** and **Id** implies a significant decrease in steric energy in shifting from the monomeric to the dimeric structure for these shorter ligands.

(34) Kunkel, G. J.; Busch, K. L. *Abstracts of Papers*; *41st Conference on Mass Spectrometry and Allied Topics*; San Francisco, CA, May 31–June 4, 1993; ASMS, Elsevier Science, Inc.: New York, 1993; pp 996a,b.

(35) Thölmann, D.; McMahon, T. B. *Abstracts of Papers*: *41st Conference on Mass Spectrometry and Allied Topics*; San Francisco, CA, May 31–June 4, 1993; ASMS, Elsevier Science, Inc.: New York, 1993; pp 1002a,b.

Table 3. Calculated Steric Energies for the 1:1 Iron(III) Dihydroxamate Complexes[a]

ligand	E_m[b]	E_d[c]	ΔE_{calc}[d]
Ia	9	14	−4
Ib	10	13	−7
Ic	20	13	−27
Id	56	12	−100
RA	10	16	−4

[a] In kcal/mol. [b] Calculated relative steric energy of the monomer structure. [c] Calculated relative steric energy of the dimer structure.[d] For the hypothetical dimerization reaction, eq 3, $\Delta E_{calc} = E_d - 2E_m$.

Discussion

We have used ESMS to establish that for the iron(III) complexes of **I**, a shift in solution structure from monomeric to dimeric occurs upon descending from **Ia** to **Id**. It is worthwhile to consider the driving force for such a shift in structure.

We may formally consider the dimerization reaction in eq 3 to be a very simple case of ring-opening polymerization. The driving force for such a reaction lies in the ring strain relieved upon dimerization. The dimerization reaction formally may be considered to occur in two steps: (1) ring opening occurs, and then (2) two ring-opened species react to form the dimer. Therefore, the following theoretical energy terms related to the dimerization reaction may be defined.

H_m = steric enthalpy for monomeric structure

H_{bm} = iron(III) binding enthalpy for monomeric structure

S_m = entropic contribution for monomer ring opening

H_d = steric enthalpy for dimeric structure

H_{bd} = iron(III) binding enthalpy for dimeric structure

S_d = entropic contribution for dimer ring formation

The overall free energy change for the dimerization reaction is represented as the sum in eq 4. We may the assume that $2H_{bm}$

$$\Delta G_0 = H_d + H_{bd} - TS_d - 2H_m - 2H_{bm} + 2TS_m \quad (4)$$

$\approx H_{bd}$ since the binding enthalpy depends only on the nature of the iron(III) binding site. For the hypothetical reaction, eq 3, $\Delta H_3 = H_d - 2H_m$ and $\Delta S_3 = S_d - 2S_m$. The Gibbs free energy change for eq 3 now reduces to eq 5.

$$\Delta G_0 = (H_d - 2H_m) - T(S_d - 2S_m) = \Delta H_3 - T\Delta S_3 \quad (5)$$

We expect the entropic term to be significant and unfavorable but fairly constant for different n. For the reaction to be spontaneous, $\Delta H_3 < T\Delta S_3$. Therefore, the structural shift from monomeric to dimeric complexes as n decreases should be driven by steric enthalpy contributions to the reaction free energy. Examination of the calculated reaction energies based on steric considerations alone—ΔE_{calc}, Table 3—suggests the general trend for actual reaction enthalpy, ΔH_3, to become more negative as n decreases. Since the calculated steric energy for the dimeric structure, E_d, varies only slightly with n, Table 3 suggests that the driving force for the shift from monomeric to dimeric structure is the increasing steric energy in the monomeric structures as n is decreased.

The "crossover" point is where ΔH_3 and $T\Delta S_3$ are equal. In the neighborhood of the crossover point there is a finite region where the monomer and dimer may exist in equilibrium. Systems far from the crossover point, where ΔG_0 is significantly nonzero, are where a single species, the monomer *or* the dimer, strongly predominates in solution. ESMS data show that for the series of ligands **I**, the system nearest the crossover point is the iron complex of **Ib**. In Martell's series of unsubstituted (R_N = H, n = 4−8) dihydroxamic acids,[7] a decrease in n results in a decrease in overall complex stability. There is a large discontinuity in the stability constant at $n = 6$, suggesting that a shift in solution structure may be taking place in the N-*un*substituted complexes when $n = 6$.

The natural RA ligand forms a 1:1 monomer complex with iron as shown by the ESMS in Figure 7. This is reasonable since the hydroxamate groups are separated by ten atoms in RA. The amide ring may add a certain amount of rigidity to the ligand. This may result in some small strain in RA, but not sufficient to induce dimerization, consistent with the small negative value for ΔE_{calc} for RA, Table 3.

The fact that naturally occurring trihydroxamate siderophore ligands have more than six atoms separating multiple bidentate iron binding sites[16,36] is significant in light of the results reported here. It would seem that at least six methylene units are required to separate two hydroxamate groups in order to efficiently form a monomeric complex. For our ferric dihydroxamate complexes, we expect an entropic contribution favoring formation of the monomer, and only by destabilizing the monomer through steric strain does dimerization occur. We might expect that for trihydroxamate siderophores with connecting chains consisting of less than six atoms, oligomerization driven by steric strain may also occur. However, since dimerization due to steric strain requires an overall decrease in complex stability (per metal ion), it should be energetically costly, and therefore less efficient, for a microorganism to construct its hexadentate trihydroxamate siderophores in such a way as to require dimerization to fully bind the iron.

Conclusion

We have demonstrated the use of ESMS to elucidate a subtle but significant problem related to iron transport phenomena: whether the 1:1 complexes of iron and a dihydroxamic acid form monomeric or oligomeric structures. It was established that for the model series **I**, a bridging chain length of eight methylene units formed exclusively the monomer in Scheme 1. On the other hand, the ligands whose hydroxamate groups were spanned by 2 or 4 methylene units formed exclusively the dimer complex. When $n = 6$, both monomer and dimer were observed in the mass spectrum. This was intepreted in terms of ring strain, which prevents formation of the monomer for short bridging chain lengths. The natural dihydroxamic acid rhodotorulic acid, **II**, forms the monomer, with only weak evidence for the formation of a small amount of the dimer in the mass spectrum.

Acknowledgment. We are grateful for the support of the donors of the Petroleum Research Fund, administered by the American Chemical Society (A.L.C.) and the NSF (A.L.C. CHE-9113199), and the North Carolina Biotechnology Center (R.D.S.). We thank Dr. Frederick Chaubet and L. P. Cogswell, III, for assistance with the synthesis of some of the ligands used in this study.

Supplementary Material Available: Table 1 listing parameters not standard to the Tripos 5.2 force field and Figures 2−5 showing ESMS spectra of the iron(III) complex with **Ib**, **Ic**, **Id**, and RA, respectively (5 pages). Ordering information is given on any current masthead page.

(36) Winkelmann, G., Ed. *CRC Handbook of Microbial Iron Chelates*; CRC Press: New York, 1991.